A&A 495, L17–L21 (2009)
DOI: 10.1051/0004-6361/200911633
© ESO 2009

Astronomy & Astrophysics

Letter to the Editor

Pluto's lower atmosphere structure and methane abundance from high-resolution spectroscopy and stellar occultations

E. Lellouch[1], B. Sicardy[1,2,⋆], C. de Bergh[1], H.-U. Käufl[3], S. Kassi[4], and A. Campargue[4]

[1] LESIA, Observatoire de Paris, 5 place Jules Janssen, 92195 Meudon, France
e-mail: emmanuel.lellouch@obspm.fr
[2] Université Pierre et Marie Curie, 4 place Jussieu, 75005 Paris, France
[3] European Space Observatory, Karl-Schwarzschild-Strasse 2, 85748 Garching bei München, Germany
[4] Laboratoire de Spectrométrie Physique, Université Joseph Fourier, BP 87, 38402 St-Martin d'Hères Cedex, France

Received 9 January 2009 / Accepted 29 January 2009

ABSTRACT

Context. Pluto possesses a thin atmosphere, primarily composed of nitrogen, in which the detection of methane has been reported.
Aims. The goal is to constrain essential but so far unknown parameters of Pluto's atmosphere, such as the surface pressure, lower atmosphere thermal stucture, and methane mixing ratio.
Methods. We use high-resolution spectroscopic observations of gaseous methane and a novel analysis of occultation lightcurves.
Results. We show that (i) Pluto's surface pressure is currently in the 6.5–24 μbar range, (ii) the methane mixing ratio is 0.5 ± 0.1%, adequate to explain Pluto's inverted thermal structure and ∼100 K upper atmosphere temperature, and (iii) a troposphere is not required by our data, but if present, it has a depth of at most 17 km, i.e. less than one pressure scale height; in this case methane is supersaturated in most of it. The atmospheric and bulk surface abundances of methane are strikingly similar, a possible consequence of a CH_4-rich top surface layer.

Key words. infrared: solar system – Kuiper Belt – solar system: general – planets and satellites: individual: Pluto

1. Introduction

Since its detection in the 1980s (Brosch 1995; Hubbard et al. 1988; Elliot et al. 1989), stellar occultations have revealed remarkable features in Pluto's tenuous (μbar-like) atmosphere. Pluto's upper atmosphere is isothermal ($T \sim 100$ K at altitudes above 1215 km from Pluto's center) and has undergone a pressure expansion by a factor of 2 from 1988 to 2002, probably related to seasonal cycles, followed by a stabilization over 2002–2007 (Sicardy et al. 2003; Elliot et al. 2003, 2007; E. Young et al. 2008). Below the 1215 km level, occultation lightcurves are characterized by a sharp drop ("kink") in flux, interpreted as due to either a ∼10 km-thick thermally inverted layer (stratosphere) or absorption by a low-altitude haze with significant opacity (>0.15 in vertical viewing). So far, observations of stellar occultations have provided no constraints on the atmospheric structure at deeper levels, nor on the surface pressure.

While Pluto's atmosphere is predominantly composed of N_2, the detection of methane has been reported from 1.7 μm spectroscopy (Young et al. 1997), leading to a rough estimate of the CH_4 column density (1.2 cm-am within a factor of 3–4). Even before its detection, methane had been recognized as the key heating agent in Pluto's atmosphere, able to produce a sharp thermal inversion (Yelle & Lunine 1989; Lellouch 1994; Strobel et al. 1996). The large uncertainty in the data of Young et al., however, as well as the unknown N_2 column density, did not allow one to determine the CH_4 / N_2 mixing ratio.

We here report on high-quality spectroscopic observations of gaseous CH_4 on Pluto, from which we separately determine the column density and equivalent temperature of methane. Combining this information with a novel analysis of recent occultation lightcurves, we obtain a precise measurement of the methane abundance, as well as new constraints on the structure of Pluto's lower atmosphere and the surface pressure.

2. VLT/CRIRES observations

Observations of Pluto were obtained with the cryogenic high-resolution infrared echelle spectrograph (CRIRES, Käufl et al. 2004) installed on the ESO VLT (European Southern Observatory Very Large Telescope) UT1 (Antu) 8.2 m telescope. CRIRES was used in adaptive optics mode (MACAO) and with a 0.4″ spectrometer slit. The instrument consists of four Aladdin III InSb arrays. We focused on the 2 ν_3 band of methane, covering the 1642–1650, 1652–1659, 1662–1670, and 1672–1680 nm ranges at a mean spectral resolution of 60 000, almost five times better than in the Young et al. (1997) observations. Observations were acquired on August 1 (UT = 3.10–4.30) and 16 (UT = 0.55–2.20) 2008, corresponding to mean Pluto (East) longitudes of 299° and 179°, respectively. (We use the orbital convention of Buie et al. (1997) in which the North Pole is currently facing the Sun.) Pluto's topocentric Doppler shift was +20.0 and +24.8 km s^{-1} (i.e. ∼0.11 and ∼0.14 nm) on those two dates, ensuring proper separation of the Pluto methane lines from their telluric counterparts. On each date, we also observed one telluric standard star (HIP 91347 and HIP 87220). We emphasize the August 1 data, which have the highest quality.

⋆ Senior member of the Institut Universitaire de France.

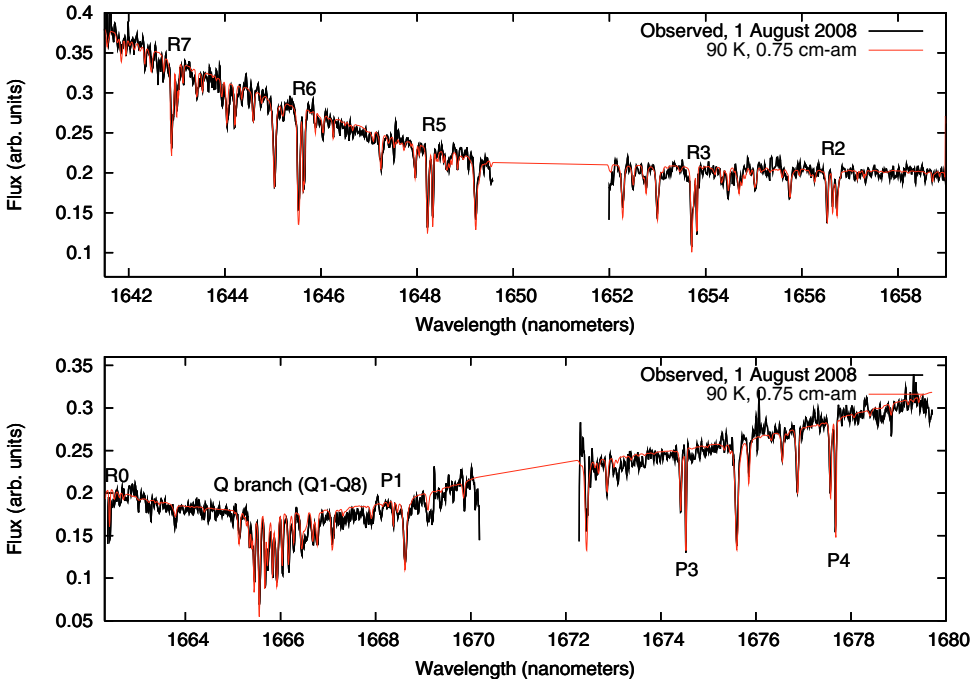

Fig. 1. Black: Pluto spectrum observed with VLT/CRIRES. Red: Best-fit isothermal model (90 K, 0.75 cm-am CH_4), including telluric and solar lines. The general continuum shape is due to absorption in the 2 ν_2 + ν_3 and 2 ν_3 bands of solid methane (see Douté et al. 1999).

3. Inferences on Pluto's lower atmosphere structure and methane abundance

The observed spectrum (Fig. 1) shows detection of no less than 17 methane lines of the P, Q, and R branches of the $2\nu_3$ band, including high J-level lines (up to R7 and Q8), and, more marginally, the presence of a few weaker lines belonging to other band(s) of methane (see below). This spectral richness makes it possible to separate temperature and abundance effects in the Pluto spectra for the first time.

Spectra were directly modelled using a telluric transmission spectrum checked against the standard star observations, a solar spectrum (Fiorenza & Formisano 2005) and a line-by-line synthetic spectrum of Pluto. The three components were shifted according to their individual Doppler shifts, and then convolved to the instrumental resolution of 60 000, determined by fitting the width of the telluric lines (and corresponding to an effective source size of 0.33″). For modelling the Pluto spectrum, we used a recent CH_4 line list (Gao et al. 2009), based on laboratory measurements (positions and intensities) at 81 K and including lower energy levels for 845 lines, determined by comparison with the intensities at 296 K collected in the HITRAN database. Although the temperature of laboratory data is similar to Pluto's, we used only lines for which energy levels were available, in order to avoid dubious extrapolation towards lower temperatures. These data show that, in addition to the J-manifolds of the $2\nu_3$ band, the spectral range contains other lines with a low energy level (e.g. $J = 2$ near 6085.2 cm^{-1}, see Fig. 2), which appear to be marginally detected in the Pluto spectrum (see Fig. 3).

3.1. Isothermal fits

We first modelled the data in terms of a single, isothermal methane layer. Because collisional broadening is negligible at the low pressures of Pluto's atmosphere, results at this step are independent of Pluto's pressure-temperature structure.

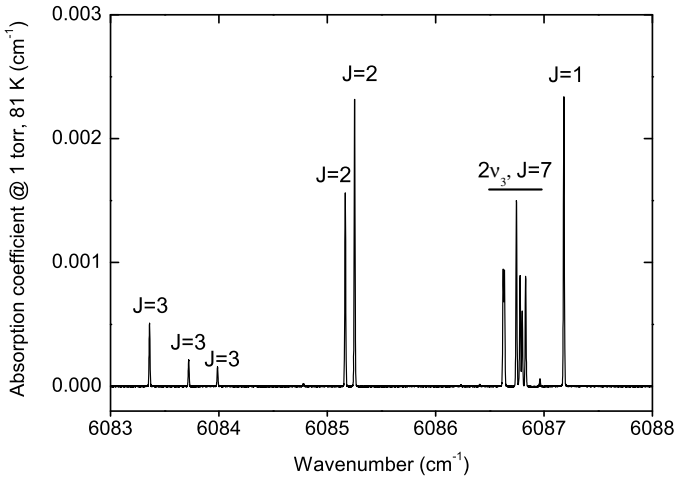

Fig. 2. Laboratory spectrum of methane at 81 K in the 6083–6088 cm^{-1} range, demonstrating the existence of strong, low J-level lines in addition to the R-branch manifolds of the $2\nu_3$ band. The J-level for these lines is determined by comparing their intensity at 81 K and at room temperature (see Gao et al. 2009). The $J = 2$ doublet near 6085.2 cm^{-1} is marginally detected in the Pluto spectrum (1643.4 nm, see Fig. 3).

Scattering was ignored, as justified below. The outgoing radiation was integrated over angles, using the classical formulation in which the two-way transmittance is expressed as $2E_2(2\tau)$, where τ is the zenithal optical depth of the atmosphere. A least-square analysis of the data was performed in the temperature (T), column density (a) space. Figure 3 shows that the best fit of the 2008 August 1 data is achieved for $T = 90$ K. Temperatures too low (resp. too high) lead to an underestimation (resp. overestimation) of the high-J lines and an overestimation (resp. underestimation) of the low-J lines. Based on least-square fitting, we inferred $T = 90^{+25}_{-18}$ K and $a = 0.75^{+0.55}_{-0.30}$ cm-am

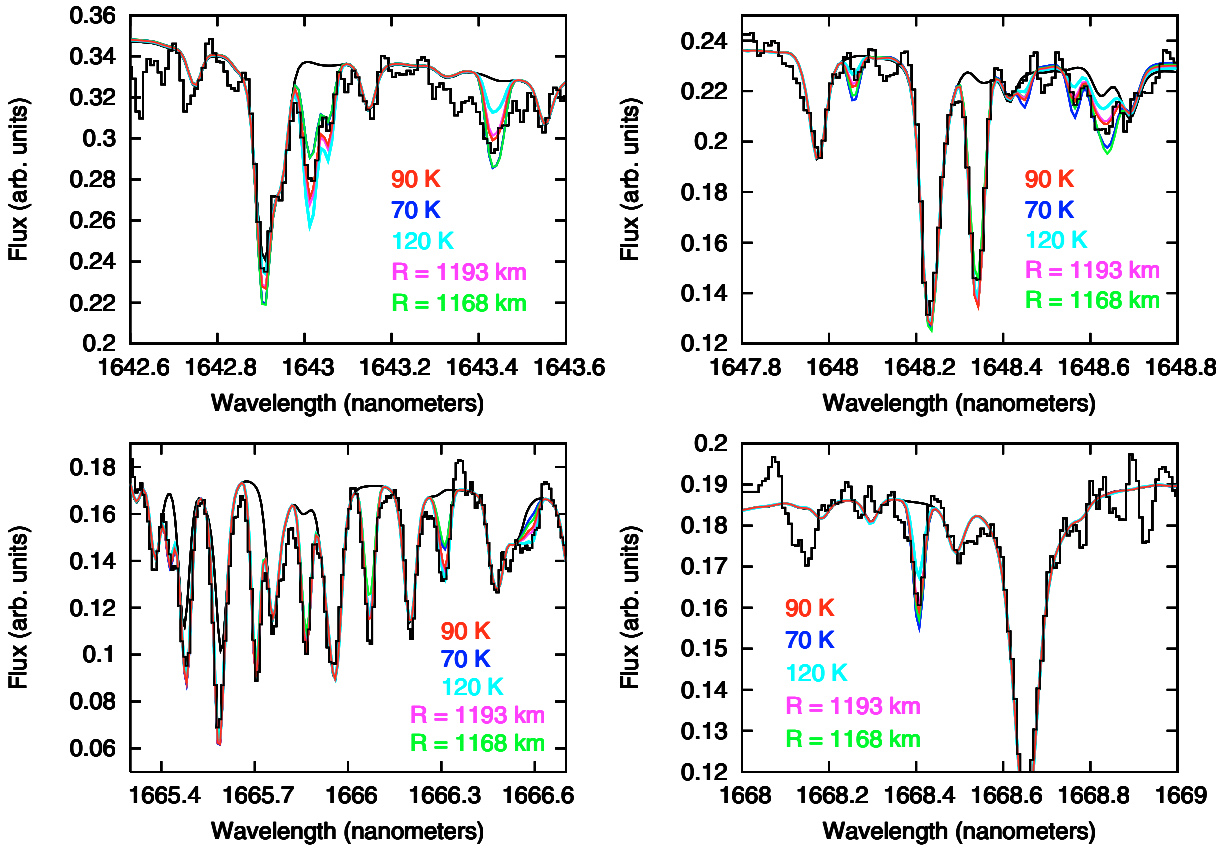

Fig. 3. Model fitting of the 2008, August 1 Pluto spectrum (histograms) zoomed on four spectral regions. The black curve is a model with no methane on Pluto. The 90 K, 70 K, and 120 K curves indicate isothermal, single-layer, fits, including 0.75 cm-am, 1.3 cm-am and 0.45 cm-am of CH_4, respectively. The rotational distribution of lines indicates that a 90 K temperature provides the best fit. The "R = 1193 km" model (pink, fit almost indistinguishable from the 90 K model) corresponds to a 6 K/km stratospheric temperature gradient, a 1193 km radius (7.5 μbar surface pressure) and a 0.62% methane mixing ratio. The "R = 1168 km" model includes a 6 K/km stratospheric temperature gradient, joining with a wet tropospheric lapse rate of –0.1 K/km below 1188 km (tropopause) and extending down to a 1168 km surface radius (29 μbar). This 20 km-deep troposphere model, optimized here with CH_4 = 0.36%, is inconsistent with the methane spectrum; for this thermal profile, the minimum radius is 1172 km (see Fig. 4). The wavelength scale is in the observer frame. These spectral regions are those showing maximum sensitivity to the methane temperature (or equivalently depth of the troposphere), as they include low J-level and high J-level lines, but for quantitative analysis, a least-square fit on all lines was performed.

for the August 1 data, and similar numbers ($T = 80^{+25}_{-15}$ K and $a = 0.65^{+0.35}_{-0.30}$ cm-am) for August 16.

3.2. Combination with inferences from stellar occultations

The above inferred methane temperatures, much warmer than Pluto's mean surface temperature (~50 K, Lellouch et al. 2000) are inconsistent with a deep, cold and methane-rich troposphere, such as the ~40 km troposphere advocated to match estimates of Pluto's radius from the Pluto-Charon mutual events (Stansberry et al. 1994). To quantify this statement, we combined our spectroscopic data with a new assessment of stellar occultation lightcurves. Besides the isothermal part and the "kink" feature mentioned previously, recent high-quality, occultation curves (Sicardy et al. 2003; Elliot et al. 2003, 2007; E. Young et al. 2008; L. Young et al. 2008) exhibit several remarkable characteristics: (i) a low residual flux during occultation, typically less than 3% of the unattenuated stellar flux; (ii) the conspicuous absence of caustic spikes in the bottom part of the lightcurves; (iii) the existence of a central flash caused by Pluto's limb curvature, in occultations in which the Earth passed near the geometric center of the shadow.

To determine the range of Pluto's thermal structures that can account for these features, we performed ray-tracing calculations for a variety of temperature/pressure profiles, expanding upon the work of Stansberry et al. (1994). For this task, we assumed a clear atmosphere. This is justified by (i) the absence of color variation in the central flash (L. Young et al. 2008); and (ii) the difficulty of hazes being produced photochemically at the required optical depth in a tenuous atmosphere like Pluto's (Stansberry et al. 1989). We thus adopted the "stratospheric gradient" interpretation of the lightcurves, and explored a broad range of situations, varying the value of this gradient, the level at which the inversion layer connects to a troposphere (i.e. the tropopause pressure), and the depth and lapse rate of this troposphere (Fig. 4).

We reached the following conclusions (Figs. 4 and 5): (i) the stratospheric temperature gradient is in the 3–15 K/km range. Gradients smaller than 3 K/km would lead to residual fluxes in excess of 3%; gradients larger than 15 K/km produce residual fluxes lower than 1%, and are not even expected from radiative models (Strobel et al. 1996); (ii) within this range, the central flash implies a minimum atmospheric pressure of 7.5 ± 1.2 μbar; (iii) the absence of caustic spikes in the region of low residual flux puts stringent constraints on a putative troposphere. In most cases, it restricts such a troposphere to be at most shallow (2–5 km deep, depending on its mean temperature), and the surface pressure to less than ~10 μbar. An exception is the family of

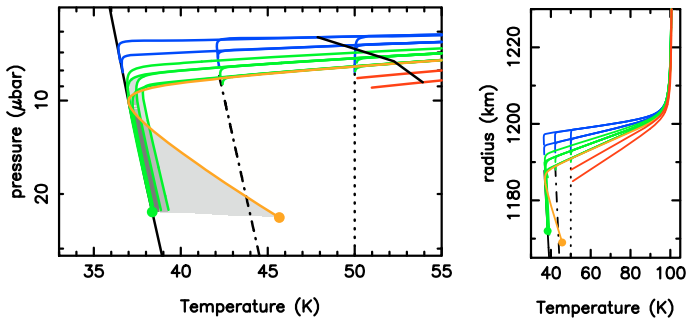

Fig. 4. Range of possible thermal profiles (pressure-temperature (*left*) and radius-temperature (*right*)) in Pluto's atmosphere. *From bottom to top*, they have stratospheric thermal gradients of 3 and 4 K/km (red profiles), 5 K/km (one orange and one green), 6 K/km (two green), 7 K/km (green), and 9 and 15 K/km (blue). All profiles are continuous in first and second order temperature derivatives. Most of these profiles have very limited tropospheres (less than 5 km in depth) or none at all, in order to match the residual flux observed during stellar occultations and avoid the formation of strong caustics (see Fig. 5). Only profiles in green and orange, with moderate stratospheric temperature gradients (5–7 K/km) and a cold tropopause (<38 K), can have significant tropospheres. The lapse rate in such tropospheres ranges from –0.1 K/km, corresponding to the N_2 wet adiabat (green profiles) to –0.6 K/km (N_2 dry adiabat, orange profile). The CRIRES spectra indicate that these wet and dry profiles cannot extend deeper than $p \sim 24$ μbar (1172 and 1169 km, respectively). In the *left panel*, the solid line on the *top right* is the locus of minimum atmospheric pressure implied by the observation of a central flash, and the solid line on the left is the vapor pressure equilibrium of N_2. The dashed-dotted line is the vapor pressure equilibrium of CH_4 for a 0.5% mixing ratio. The dotted line at 50 K illustrates the maximum possible near-surface gas temperature. The shaded areas represent the range of possible tropospheres. If Pluto has a troposphere, methane must be supersaturated over most of it.

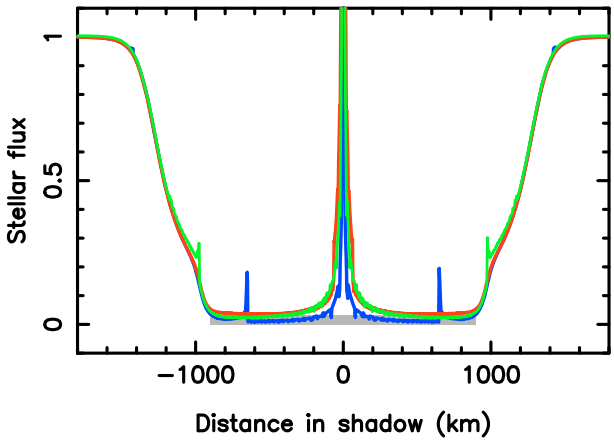

Fig. 5. Ray-tracing calculations of occultation lightcurves for representative temperature profiles of Fig. 4. The shaded area near the *bottom* of the lightcurve represents the range of residual flux (0.00–0.032) observed in the 2002, August 21 CFHT occultation (Sicardy et al. 2003), with a closest approach to shadow center of 597 km. (We estimate that the AAT June 12, 2006 occultation lightcurve (E. Young et al. 2008) consistently indicates a 0.01–0.03 residual flux). Red: lightcurve for the thermal profile with 3 K/km stratospheric gradient of Fig. 4, extending to 9 μbar. This "stratosphere-only" model is consistent with observed lightcurves. Blue: lightcurve for the thermal profile with 15 K/km stratospheric gradient, and a 4-km deep troposphere at ~36.5 K. This profile produces an unacceptable caustics spike, caused by the secondary ("far limb") image Green: light-curve for a thermal profile with 6 K/km gradient in the inversion layer, joining the N_2 saturation vapor pressure with a ~–0.1 K/km gradient in the troposphere. In this case, modest caustics are still produced, but they appear near the light-curve "kink".

thermal profiles with intermediate (5–7 K/km) stratospheric temperature gradients and a cold (<38 K) tropopause, which appear consistent with occultation curves for any tropospheric depth. In fact, such profiles (green curves in Figs. 4 and 5) lead to modest caustic spikes in the region of the "kink", i.e. where spikes are observed in actual observations, for which they can be mistaken.

The allowed thermal profiles were finally tested against the methane spectrum. We assumed uniform atmospheric mixing, which is a plausible case given that (i) the source of methane is at the surface; (ii) its equivalent temperature implies that a large fraction of methane is in the upper atmosphere, and performed a least-square analysis of the data in the (surface radius, CH_4 mixing ratio) domain. Not surprisingly in view of the isothermal fits, thermal profiles having no (or a mini-) troposphere are all consistent with the methane spectrum. For example, for a stratospheric temperature gradient of 6 K/km, a surface radius of 1193 km (surface pressure = 7.5 μbar, i.e. the minimum required by the occultations) provides an adequate fit of the August 1 data for a CH_4 mixing ratio of 0.62%. In contrast, profiles including too deep a troposphere can be rejected as giving too much weight to cold methane and leading to a line distribution inconsistent with the data. Based on such fits, the maximum tropospheric depth is found to be 17 km (i.e. 0.85 pressure scale heights) and the maximum surface pressure is 24 μbar. Taking all constraints together, Pluto's surface pressure in 2008 is in the range 6.5–24 μbar. The range of methane column densities is 0.65–1.3 cm-am. Deeper (i.e. colder) models require larger methane columns than the more shallow models, but since they also have a higher surface pressure, the methane mixing ratio is accurately determined to be 0.51 ± 0.11%. Constraints from the August 16 data are somewhat looser (a maximum surface pressure and troposphere depth of 32 μbar and 23 km, respectively). The minimum Pluto radius implied by the data is 1169–1172 km (Fig. 4). This value holds for the nominal astrometric solutions for stellar occultations, typically uncertain by ~10 km. Given this uncertainty, our lower limit on the radius is consistent with most inferences from the mutual events (nominally 1151–1178 km, see Tholen et al. 1997). The troposphere depth is free of this uncertainty, hence better constrained than Pluto's radius.

4. Discussion

4.1. Methane mixing ratio and possible supersaturation

Through absorption of solar input in the near-IR and radiation at 7.7 μm, methane is the key heating/cooling agent in Pluto's atmosphere, and in particular, it must be responsible for its thermal inversion. Detailed calculations (Strobel et al. 1996) show that, even in the presence of CO cooling and for an assumed 3 μbar "surface" (i.e. base of the inversion layer) pressure, a 0.3% methane mixing ratio produces a 7 K/km "surface" gradient and a temperature increase of ~36 K in the first 10 km. Although such calculations will need to be redone in the light of our results, a 0.5% methane mixing ratio is clearly adequate to explain the ~6 K/km gradient indicated by the occultation data, further justifying our assumption of neglecting haze opacity.

The presence of methane in Pluto's stratosphere implies that it is not severely depleted by atmospheric condensation. Nevertheless, a remarkable result is that for models including a troposphere, methane appears to be significantly supersaturated (Fig. 4), by as much as a factor ~30 for a ~38 K tropopause. Given that Pluto's troposphere is at its most shallow (less than

1 pressure scale height), this plausibly results from convective overshoot associated with dynamical activity, combined with a paucity of condensation nuclei in a clear atmosphere.

4.2. The origin of the elevated methane abundance

In agreement with Young et al. (1997), the CH_4/N_2 mixing ratio we derive is orders of magnitude greater than the ratio of their vapor pressures at any given temperature, and the discrepancy is even worse if one considers that methane is a minor component on Pluto's surface. Two scenarios (Spencer et al. 1997; Trafton et al. 1997) have been described to explain this elevated methane abundance: (i) the formation, through surface-atmosphere exchanges, of a thin methane-rich surface layer (the so-called "detailed balancing" layer), which inhibits the sublimation of the underlying, dominantly N_2, frost, and leads to an atmosphere with the same composition as this frost; (ii) the existence of geographically separated patches of pure methane, warmer than nitrogen-rich regions, that under sublimation boost the atmospheric methane content. Interestingly, detailed analyses of 1.4–2.5 μm and 1–4 μm mid-resolution spectra give observational credit to both situations. It is noteworthy that our 0.5% atmospheric abundance is identical to the CH_4/N_2 ratio in the N_2 – CH_4 – CO subsurface layer of Douté et al. (1999), consistent with the detailed balancing model, and also agrees with the solid methane concentration inferred by Olkin et al. (2007) (0.36%). In this framework, a typical 15 μbar surface pressure could be explained if the N_2 – CH_4 – CO subsurface layer is at 40.5 K (consistent with the N_2 ice temperature measurements of Tryka et al. 1994) and overlaid by a 80% CH_4 – 20% N_2 surface layer. On the other hand, and in favor of the alternate scenario, thermal IR lightcurves (Lellouch et al. 2000), as well as sublimation models for CH_4 (Stansberry et al. 1996), indicate that extended pure CH_4 patches may reach dayside temperatures well in excess of 50 K. This is more than sufficient to explain the ~0.075 μbar CH_4 partial pressure indicated by our data.

Distinguishing between the two cases may rely on the time evolution of the N_2 pressure and CH_4 mixing ratio. In particular, the decrease in atmospheric CH_4 with increasing heliocentric distance is expected to lead to a drop in the CH_4 abundance in the detailed balancing layer, which may delay the decrease in the N_2 pressure (Trafton et al. 1998). Assuming T = 100 K, Young et al. (1997) reported a 0.33–4.35 cm-am methane abundance in 1992. Although their error bars are very large, their best-fit value (1.2 cm-am) is higher than ours (0.65 cm-am for this temperature). Combined with the factor of ~2 pressure increase between 1988 and 2002, this suggests that the methane mixing ratio is currently declining. The ALICE and Rex instruments on *New Horizons* will measure Pluto's surface pressure and methane abundance in 2015. Along with the data presented in this paper, this will provide new keys to the seasonal evolution of Pluto's atmosphere and the surface-atmosphere interactions.

Acknowledgements. This work is based on observations performed at the European Southern Observatory (ESO), proposal 381.C-0247. We thank Darrell Strobel for constructive reviewing.

References

Brosch, N. 1995, MNRAS, 276, 571
Buie, M. W., Tholen, D. J. & Wasserman, L. H. 1997, Icarus, 125, 233
Douté, S., Schmitt, B., Quirico, E., et al. 1999, Icarus, 142, 421
Elliot, J. L., Dunham, E. W., Bosh, A. S., et al. 1989, Icarus, 77, 148
Elliot, J. L., Ates, A., Babcock, B. A., et al. 2003, Nature, 424, 165
Elliot, J. L., Person, M. J., Gulbis, A. A. S., et al. 2007, Astron. J., 134, 1
Fiorenza, C., & Formisano, V. 2005, Planet. Space Sci., 53, 1009
Gao, B., Kassi, S., & Campargue, A. 2009, J. Mol. Spectro, 253, 55
Hubbard, W. B., Hunten, D. M., Dieters, S. W., et al. 1988, Nature, 336, 452
Kaeufl, H.-U., Ballester, P., Biereichel, P., et al. 2004, SPIE, 5492, 1218
Lellouch, E. 1994, Icarus, 108, 225
Lellouch, E., Laureijs, R., Schmitt, B., et al. 2000, Icarus, 147, 220
Olkin, C. B., Young, E. F., Young, L. A., et al. 2007, Astron. J., 133, 420
Sicardy, B., Widemann, T., Lellouch, E., et al. 2003, Nature, 424, 168
Spencer, J. R., Stansberry, J. A., Trafton, L. M., et al. 1997, in Pluto and Charon, ed. S. A. Stern, & D. J. Tholen (The University of Arizona Press), 435
Stansberry, J. A., Lunine, J. I., & Tomasko, M. G. 1989, GRL, 16, 1221
Stansberry, J. A., Lunine, J. I., Hubbard, W. B., et al. 1994, Icarus, 111, 503
Stansberry, J. A., Spencer, J. R., Schmitt, B., et al. 1996, Planet. Space Sci., 44, 1051
Strobel, D. F., Zhu, X., & Summers, M. E. 1996, Icarus, 120, 266
Tholen, D. J., & Buie, M. W. 1997, in Pluto and Charon, ed. S. A. Stern, & D. J. Tholen (The University of Arizona Press), 193
Trafton, L. M., Hunten, D. M., Zanhle, K. J., & McNutt, R. L. 1997, in Pluto and Charon, ed. S. A. Stern, & D. J. Tholen (The University of Arizona Press), 475
Trafton, L. M., Matson, D. L., & Stansberry, J. A. 1998, in Solar System Ices, ed. B. Schmitt, C. de Bergh, & M. Festou (Kluwer Academic Publishers), 773
Tryka, K. A., Brown, R. H., Chruikshank, D. P., et al. 1994, Icarus, 112, 513
Yelle, R. V., & Lunine, J. I. 1989, Nature, 399, 288
Young, L. A., Elliot, J. L., Tokunaga, A., et al. 1997, Icarus, 127, 258
Young, E. F., French, R. G., Young, L. A., et al. 2008, Astron. J., 136, 1757
Young, L., Buie, M. W., Olkin, C. B., et al. 2008, Bull. Amer. Astron. Soc. 40, 461